

Deeply Virtual Compton Scattering at 11 GeV in Jefferson Lab Hall A

Frédéric Georges*†

Institut de Physique Nucléaire d'Orsay

E-mail: georges@ipno.in2p3.fr

Introduced in the mid 90's, Generalized Parton Distributions (GPDs) are now a key element in the study of the nucleon internal structure. Indeed, GPDs encapsulate both spatial and momentum distributions of partons inside a nucleon, and through the Ji sum rule, they also allow to derive the total orbital angular momentum of quarks.

GPDs are experimentally accessible through Deeply Virtual Compton Scattering (DVCS) and its interference with the Bethe-Heitler process at high momentum transfer Q^2 . A worldwide experimental program was started in the early 2000's to extract these GPDs. The subject of this document, a DVCS $ep \rightarrow e\gamma$ experiment performed at Jefferson Laboratory, Hall A (Virginia, USA) between 2014 and 2016, is encompassed in this program.

The aim of this experiment is to extract the DVCS helicity-dependent cross sections as a function of the momentum transfer Q^2 , for fixed values of the Bjorken variable x_B , on a proton target. The recent upgrade of the accelerator facility to 12 GeV allows to cover a larger lever arm in Q^2 than for previous measurements, while the polarized electron beam will allow the separation of the contributions from the real and imaginary parts of the DVCS amplitude to the total cross section. This document will present an overview of the ongoing data analysis for this experiment.

XVII International Conference on Hadron Spectroscopy and Structure

25-29 September, 2017

University of Salamanca, Salamanca, Spain

*Speaker.

†For the Jefferson Lab Hall A collaboration

1. Accessing Generalized Partons Distributions through Deeply Virtual Compton Scattering

A large number of experiments have already been made in order to study the internal structure of the proton. Elastic scattering $ep \rightarrow ep$ gives access to elastic form factors, which provide information about the spatial distribution of partons inside of the proton. Deep Inelastic Scattering (DIS) $ep \rightarrow eX$ gives access to partons distribution functions, which yield information about the momentum distribution of partons inside of the proton. However, the disadvantage of such measurements is that they cannot provide information about the correlations between spatial and momentum distributions of partons, and as such, our understanding of the proton internal structure remains incomplete.

In the early 2000's, the Deeply Virtual Compton Scattering (DVCS) $ep \rightarrow ep\gamma$ process started to gather a lot of interest, as it is one of the cleanest ways to extract Generalized Partons Distributions (GPDs). Indeed, introduced in the mid 90's, GPDs are providing essential information for the study of the proton internal structure, since they give access to the correlations between spatial and momentum distributions of partons, as well as the total orbital angular momentum of quarks through the Ji sum rule [1, 2, 3].

In the Bjorken limit (Eq. 1.1), the DVCS process can be simplified to the 'Handbag diagram' (see fig. 1), where an electron is scattering off a single quark of the proton through the exchange of a virtual photon, and after the interaction, the struck quark emits a real photon. This diagram can be factorized into two parts [4, 5] : a hard part (top half of Fig. 1) which can be computed with perturbative QCD, and a soft part (bottom half of Fig. 1) which is parametrized by four quark GPDs. As a consequence, the measurement of the cross section of this process allows one to extract the GPDs.

$$Q^2 = -q^2 \rightarrow \infty \quad ; \quad \nu \rightarrow \infty \quad ; \quad x_B = \frac{Q^2}{2M\nu} \quad \text{fixed} \quad (1.1)$$

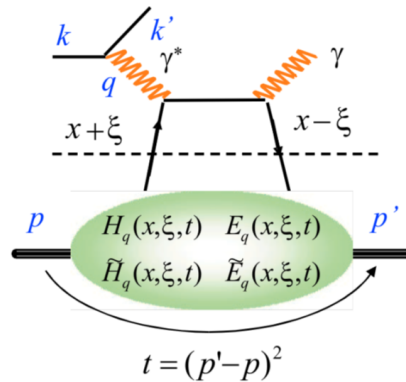


Figure 1: Handbag diagram of the DVCS process. k and k' are the electron four-vectors, p and p' are the proton four-vectors, and q is the virtual photon four-vector. ν is the difference of energy of the electron before and after the interaction. t is the momentum transfer to the proton. $x + \xi$ and $x - \xi$ are the fractions of the proton longitudinal momentum carried by the struck quark before and after the interaction, respectively.

Experimentally, it is not possible to distinguish DVCS from the Bethe-Heitler process since they have the same initial and final state, though, in the Bethe-Heitler case, the real photon is emitted by the electron instead of a quark. As a consequence, the cross section measured experimentally has inevitably contributions from DVCS, Bethe-Heitler and an interference term. However, Bethe-Heitler is well known within 1% and by using a longitudinally polarized electron beam, at leading twist, the sum and difference of polarized cross sections allow to separate the real and imaginary parts of the DVCS amplitude:

$$d^5\vec{\sigma} - d^5\overleftarrow{\sigma} = \mathcal{I}m(T^{BH} \cdot T^{DVCS}) \quad (1.2)$$

$$d^5\vec{\sigma} + d^5\overleftarrow{\sigma} = |BH|^2 + \mathcal{R}e(T^{BH} \cdot T^{DVCS}) + |DVCS|^2 \quad (1.3)$$

2. Experiment goal and apparatus

The data acquisition of the experiment took place at Jefferson Lab (Newport News, Virginia, USA), in Hall A, between Fall 2014 and Fall 2016. This experiment has two main goals : perform a scaling test with a larger Q^2 lever arm than before, for several values of x_B (see Fig. 2), and separate the real and imaginary parts of the DVCS amplitude (see Eq. 1.2 and 1.3) [6].

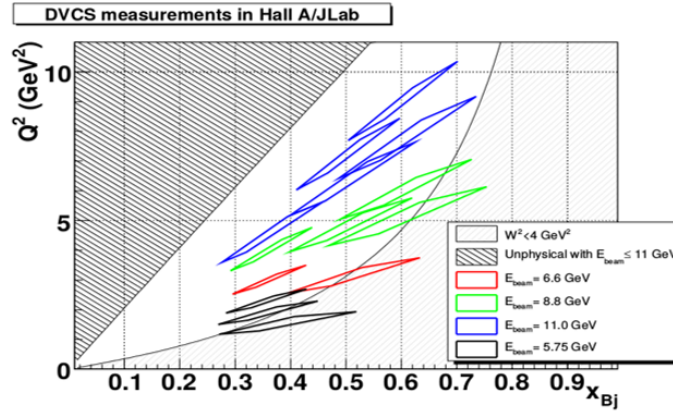


Figure 2: The kinematic regions (Q^2 ; x_B) explored by this DVCS experiment are represented in red, green and blue. The regions in black were studied during a previous experiment, in 2010.

A longitudinally polarized electron beam was sent on a liquid hydrogen target. The scattered electron was detected in a High Resolution Spectrometer (HRS) [7] while the emitted photon was detected in a custom electromagnetic calorimeter made of 208 PbF₂ crystals. The recoil proton was not detected, however, it was identified by the missing mass $ep \rightarrow eX\gamma$: $M_x^2 = (k + p - k' - \gamma)^2$.

3. Analysis overview

3.1 Beam polarization measurement

The electron beam longitudinal polarization has been monitored during the experiment through two methods. The first method is a Moller polarization measurement, which relies on the scattering

of the electron beam off the atomic electrons of a polarized iron target. The second method is a Compton polarization measurement, which relies on the scattering of the electron beam off the photons of a circularly polarized laser. The left/right counting asymmetries of these processes both give access to the beam polarization [7].

The data analysis of the Compton measurements is still in progress, however, preliminary results of the combined Compton and Moller measurements show a high beam polarization of $\sim 85\%$, with a good stability.

3.2 Spectrometer optics calibration

At the beginning of the Spring 2016 run, it was discovered that one of the supraconducting magnets of the spectrometer could no longer run at its usual setting, degrading significantly its optics. This magnet was changed before the Fall 2016 run. As a consequence, several calibrations of the spectrometer optics have been necessary.

After calibration of the optics, we reached a vertex resolution of 3.5 mm at 15.18 deg, and a relative momentum resolution of 10^{-3} .

3.3 Spectrometer acceptance study

The degradation of the magnet properties also had an effect on the acceptance of the spectrometer, which needed to be redefined. In order to do so, we used an 'R-function', which computes the distance, called 'R-value', of each event to the edges of its acceptance.

The reason for using this R-function to cut on the edges of the spectrometer 4-dimensional acceptance, instead of applying individual 1-dimensional cuts on each variable, is because some of them are correlated (see Fig. 3). Using the R-function allows for a more efficient cut.

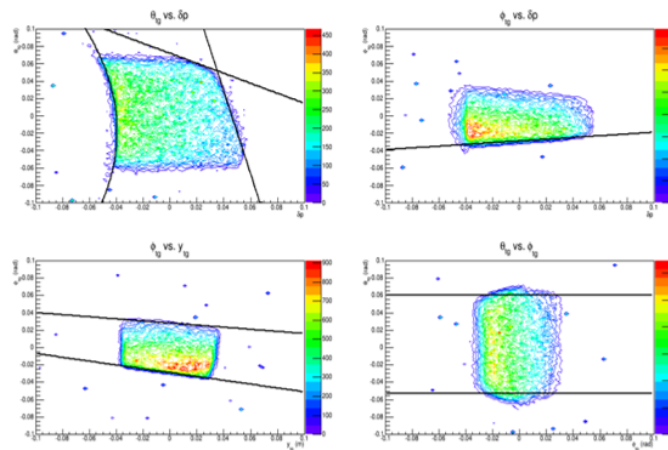


Figure 3: Projections of the 4-dimensional acceptance of the spectrometer. Top left : vertical scattering angle against momentum. Top right : horizontal scattering angle against momentum. Bottom left : horizontal scattering angle against vertex position. Bottom right : vertical against horizontal scattering angle. The black lines are the edges of the spectrometer acceptance used in the R-function.

3.4 Coincidence time correction

The coincidence time between the electron and the photon is a very important parameter. A very good resolution is necessary in order to separate accidental events and noise from DVCS events. Several corrections are applied to account for:

- The relative time between the calorimeter and the spectrometer triggers.
- The relative time among the calorimeter blocks.
- The relative time among the scintillator paddles that trigger the spectrometer.
- The photon travel time in the scintillator paddles.
- The electron time of flight through the spectrometer.

The combination of all these corrections improves the coincidence time resolution from 6.6 ns to 0.85 ns, which will allow a clear identification of DVCS events from accidentals and noise.

3.5 Calorimeter energy calibration

The limiting factor of this experiment is the calorimeter energy resolution. In order to calibrate the gain of the calorimeter, we took dedicated elastic $ep \rightarrow ep$ data. The proton which was detected in the spectrometer allowed to compute the energy of the electron detected in the calorimeter. The calibration then consists on adjusting the gain of each channel so that the reconstructed electron energy agrees with the expected value. An energy resolution of 3.6% at 4.2 GeV was obtained.

However, due to radiation damage, the calorimeter gain decreased progressively during the experiment. The previous calibration method, being invasive and long to perform, could not be used often enough to compensate its loss of gain. As a consequence, a second calibration method was used : the gains were adjusted by reconstructing the invariant mass of π^0 events $ep \rightarrow ep\pi^0$. This non invasive method was successfully used on a daily basis to compensate the calorimeter radiation damage (see Fig. 4).

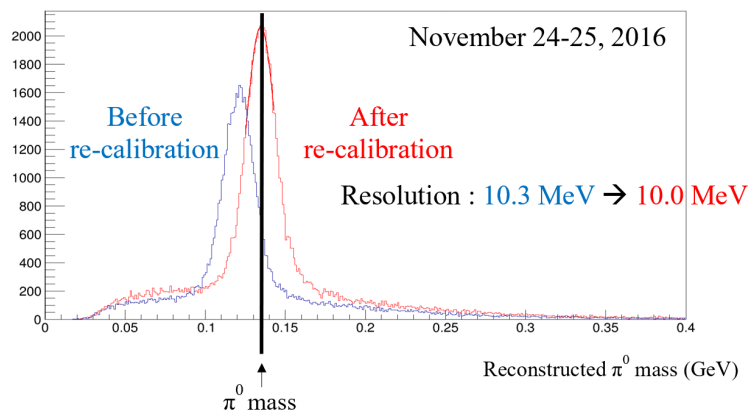


Figure 4: Reconstructed 2- γ invariant mass before (blue) and after (red) re-calibration of the calorimeter gain using the π^0 calibration method, for data taken between November 24 and November 25 of 2016. The loss of gain due to radiation damage was successfully corrected for.

3.6 Dead Time study

In order to compute the dead time of this DVCS experiment, we used scalers:

$$Deadtime = 1 - Livetime \quad ; \quad Livetime = \frac{live_scaler_rate}{scaler_rate} \quad (3.1)$$

'live scaler' designating a scaler incrementing only when the data acquisition is not busy.

In order to test this dead time computation, dedicated runs have been taken varying the electron beam current. The electrons rate in the spectrometer, normalized by the beam current, and corrected by the dead time, turned out to be independent of the beam current. This is a strong indication of a good computation of the dead time. Studies are ongoing to test these results with DVCS event rates instead of simple electron rates.

4. Outlook

The data acquisition of this experiment ended in Fall 2016 with good statistics. The analysis is currently making good progress, since all calibrations have been completed, as well as many corrections and preliminary studies. The main remaining steps are the extraction of DIS cross sections, the computation of the experiment acceptance with a Monte-Carlo simulation, the subtraction of the π^0 contamination, and finally the extraction of the DVCS cross sections and their systematic uncertainties.

We expect to have preliminary DVCS cross sections by mid-2018.

References

- [1] X.-D. Ji, *Gauge-Invariant Decomposition of Nucleon Spin and Its Spin-Off*, Phys. Rev. Lett. 78, 610 (1997), [hep-ph/9603249].
- [2] A.V. Radyushkin, *Nonforward parton distributions*, Phys. Rev. D 56, 5524 (1997), [hep-ph/9704207].
- [3] D. Mueller, D. Robaschik, B. Geyer, F.M. Dittes, J. Horejsi, *Wave Functions, Evolution Equations and Evolution Kernels from Light-Ray Operators of QCD* Fortsch. Phys. 42, 101 (1994) [hep-ph/9812448].
- [4] X.-D. Ji and J. Osborne, *One loop corrections and all order factorization in deeply virtual Compton scattering*, Phys. Rev. D 58, 094018 (1998), [hep-ph/9801260].
- [5] J. C. Collins and A. Freund, *Proof of factorization for deeply virtual Compton scattering in QCD*, Phys. Rev. D 59, 074009 (1999), [hep-ph/9801262].
- [6] J. Roche, C. E. Hyde-Wright, B. Michel, C. Munoz Camacho, et al. (The Jefferson Lab Hall A Collaboration) *Measurements of the Electron-Helicity Dependent Cross Sections of Deeply Virtual Compton Scattering with CEBAF at 12 GeV*, PR12-06-114, [nucl-ex/0609015].
- [7] J. Alcorn and al., *Basic instrumentation for Hall A at Jefferson Lab*, Phys. Research A 522, 294 (2004).